DYNAMIC ANALYSIS OF THE LIULIAKOVITSA TAILINGS DAM

Nikolay Kerenchev, Lena Mihova

Nikolay Kerenchev, Assist. Prof., Ph.D., Dipl.-Ing.; University of architecture, civil-engineering and geodesy – Sofia; Hr. Smirnenski 1; kerenchev@hotmail.com
Lena Mihova, Prof., Ph.D., M.Sc.; University of architecture, civil-engineering and geodesy – Sofia; Hr. Smirnenski 1; l_mihova@yahoo.com

ABSTRACT: Liulyakovitsa tailings dam with its height of about 180 m and length of 8600 m is the biggest tailing dam in the Balkans. This paper analysis the seismic behaviour of the dam based on Finite element method. Time history dynamic analyses using scaling real and synthetic earthquake accelerograms are performed. Seismic coefficients for pseudo static slope stability analyses are also determined. The seismic response of the dam is described. Based on the strength reduction technique the most significant failure mechanisms are estimated. The seismic coefficients for specific failure mechanism as a ratio of the peak average seismic acceleration of the sliding soil body and peak ground acceleration are obtained. Most of the calculations are performed using the PLAXIS 2D software for geotechnical analyses.

1. INTRODUCTION

Liulyakovitsa tailings dam is located in the central part of Bulgaria, 90 km east of Sofia, and is a structure for the Asarel-Medet mining complex. The construction of the tailings dam began in the 80 years of the last century on a rock ground at elevation +639.0 m and at present the ridge of the tailings material is at elevation +830.0 m. A construction of the tailings dam up to elevation +930,0 m is forthcoming.

(a) (b)

Fig. 1. Views of the Liulyakovitsa tailings dam: (a) from the side; (b) from above.

In the process of upgrading the embankment, insitu and laboratory tests were carried out to determine the physic-mechanical parameters of the material and their change over time. As Bulgaria falls within the earthquake zone, the analysis of the seismic slope stability of the dams is in most cases relevant for the design. Dynamic soil properties have been defined in a number of publications in the field of soil dynamics and seismic geoengineering: Das (1993) [1]; Ishihara (1996) [7]; Kramer (1996) [8]. A summary of studies in the field of soil dynamics in Bulgaria up to 2005 was done by Hamova (2005) [2], and more recent studies in this area in Bulgaria are as follows: Milev (2017-2019) [21] - [25]; Kerenchev (2012-2019) [9] - [11]; Mihova & Kerenchev (2013-2014) [19], [20]. Publications related to the examination of the dynamic properties of the material of Liuliakovitsa tailings dam have been made by the authors: Kerenchev (2019) [12]; Kerenchev & Milev (2019) [13]. The determination of the variable seismic coefficient for the slope stability estimation, which depends on the geometry and location of the potential slip surface, was done by Kerenchev et al. (2018) [14]. Pseudostatic approach is a traditional engineering approach for the examination of the slope stability of dams and the ground bearing capacity. It is included in the current design standards in Bulgaria and aspects of its application are discussed in the publications: Kostova (2011) [15], [16], (2018) [17]; Sulay & Tanev (2016) [30]; Sulay (2019) [29]. In Eurocode 8.5, it is explicitly noted that the pdeudo-static approach is not suitable for installations where pore pressure is generated.
The results of a dynamic "time history" analysis of the Liuliakovitsa tailings dam conducted with the Plaxis 2D software are summarized here.

2. DYNAMIC ANALISYS OF THE DAM

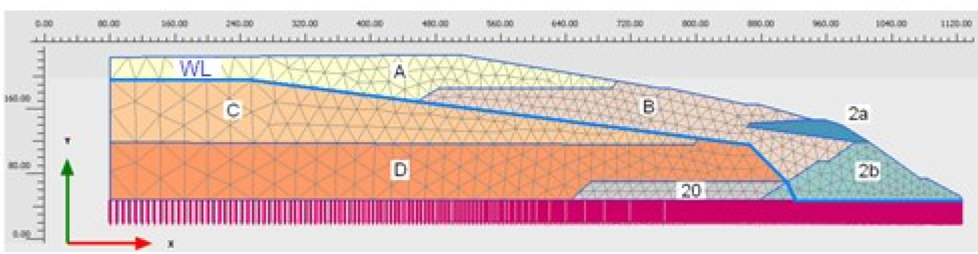

Fig. 2. Generalized model geometry and finite element mesh

In Figure 2 a 2D finite-element model for the main wall of the tailings dam is presented. The tail material is divided in 4 layers - A, B, C and D. The support prisms 2a, 2b and tongue 20 are made of rock material. For the shear modulus reduction curve as a function of shear deformations (G / G0 - γ)e and (G - γ) for the tail layers are based on the dependencies of the authors Hardin & Drnevich (1972) [3], [4] and for prisms and language - by the authors Seed & Idris (1970) [28] for gravel. The results are presented in Fig. 3, compared to the results of the authors Seed and Vucetc & Dobry (1993) [31].

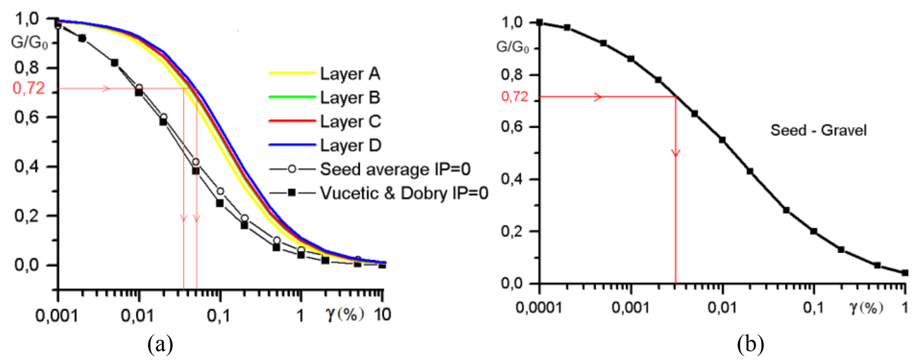

Fig. 3. G / G0 curves: (a) for the tailing material; (b) for supporting prisms and material 20

The mathematical model for dynamic analysis of the main wall is in accordance with the following premises:

- For the cross-section geometry, a multilayer model corresponding to the stages of construction of the facility (Fig. 2) is presented, as the layers are generalized in order to avoid too many refraction surfaces and reflection of seismic waves, which negatively affects the accuracy.
- The boundaries of the study area are modelled with dampers, which sufficiently absorb the seismic wave and simulate an infinite half-space of the earth base.
- The seismic action is applied by an accelerograms.

- For soil layers, an advanced elasto-plastic constitutive HS small model (Plaxis [26]) is used. The main prerequisites of this model are the following: the relation between stresses and strains is hyperbolic; stress path stiffness dependence; plastic, volumetric and deviatoric deformations are accounted; G module degrades under dynamic load; the minimum value of the G module is defined by the unloading-reloading stiffness; the Mohr-Coulomb failure criterion. The HS small model requires a significant number of material parameters as shown in Table 1 and Table 2.
- Viscous properties, friction and development of plastic deformations in soils cause the attenuation of the oscillations over time. Using the constitutive HSS model, this "internal" damping is accounted, but to a degree less than actually observed and tested in soils. The reason for this is the fact that the hyperbolic strain dependence in small deformations is close to linear and it is impossible to account for the hysteretic behaviour of the material in this zone. That's why it's required to take into account the hysteretic behaviour of the material in this area. Therefore, the introduction of additional viscous damping is required following the model of

Rayleigh (1945) [27]. Rayleigh coefficients α and β are obtained as functions of two frequencies f (Hz) at the desired attenuation factor ξ. The authors' approach is applied here: Hashash & Park (2002) [5] and Hudson, Idriss & Beirkae (2003) [6] for the first frequency to accept the first natural frequency of the soil deposit f_1 and for the second frequency - the closest odd number, greater than the ratio f_p / f_1, where fp is the predominant frequency of the input seismic signal of the Fourier spectrum. According to the literature, an additional viscous attenuation of $\xi = 5\%$ was assumed.

Table 1. Material parameters of the tailings dam material for the *HSS* constitutive model

		Layer A	Layer B	Layer C	Layer D
Natural unit weight	γ_n (kN/m^3)	19,4	19,5	19,6	20,4
Saturated unit weight	γ_r (kN/m^3)	-	-	20,4	21,5
Reference stress for stiffness	p_{ref} (kPa)	100	100	100	100
Tangent stiffness for primary oedometer loading	$E_{oed,ref}$ (kPa)	8 000	15 000	10 000	12 000
Secant stiffness in standard drained triaxial test	$E_{50,ref}$ (kPa)	8 000	15 000	10 000	12 000
Unloading/reloading stiffness	$E_{ur,ref}$ (kPa)	28 000	52 500	35 000	42 000
Initial shear modulus	$G_{0,ref}$ (kPa)	78 780	94 575	105 679	120 246
Poisson's ratio for unloading /reloading	v_{ur} (-)	0,20	0,20	0,20	0,20
Shear strains for the 0,722 of the reduction of the shear modulus*	$\gamma_{0.7}$ (%)	0,035*	0,040*	0,045*	0,050*
Power factor for the stress-level dependency of stiffness	m (-)	0,6	0,6	0,6	0,6
Coefficient of lateral earth pressure	K_0 (-)	0,577	0,47	0,546	0,5
Failure ratio	R_f (-)	0,9	0,9	0,9	0,9
Cohesion	c (kPa)	10	15	12	17
Friction angle	φ (°)	25	32	27	30

*Values are based on graph shown in Fig .3a.

- The soil layers below the water line (WL) in the tail body are modelled with non-drained behavior, which means that the bulk modulus of the two-phase soil is formed by that of the solid phase and by the bulk modulus of the water (Kw = 2.2.106 kPa)

• In the course of the dynamical action, the model generates additional pore pressure in the tail layers below the WL. The pore pressure generated does not have cumulative value over time during the earthquake. The model has the ability to register the value at any given moment that would appear at every step during the calculation. This is the reason why the resulting pore water pressure should be considered approximate.

Table 2. Material parameters of the supporting prisms and material 20 for the *HSS* constitutive model

		Layer 20	Layer 2a	Layer 2b
Natural unit weight	γ_n (kN/m^3)	22	20	20
Saturated unit weight	γ_r (kN/m^3)	-	-	-
Reference stress for stiffness	p_{ref} (kPa)	100	-	-
Tangent stiffness for primary oedometer loading	$E_{oed,ref}$ (kPa)	50 000	100	100
Secant stiffness in standard drained triaxial test	$E_{50,ref}$ (kPa)	50 000	50 000	50 000
Unloading/reloading stiffness	$E_{ur,ref}$ (kPa)	150 000	50 000	50 000
Initial shear modulus	$G_{0,ref}$ (kPa)	328 230	150 000	150 000
Poisson's ratio for unloading /reloading	v_{ur} (-)	0,2	0,20	0,20
Shear strains for the 0,722 of the reduction of the shear modulus*	$\gamma_{0.7}$ (%)	0,003**	0,003**	0,003**
Power factor for the stress-level dependency of stiffness	m (-)	0,5	0,5	0,5
Coefficient of lateral earth pressure	K_0 (-)	0,357	0,384	0,357
Failure ratio	R_f (-)	0,9	0,9	0,9
Cohesion	c (kPa)	22	22	22
Friction angle	φ (°)	40	38	40

** Values are based on graph shown in Fig .3b

• The soil layers below the water line (WL) in the tail body are modelled with non-drained behavior, which means that the bulk modulus of the two-phase soil is formed by that of the solid phase and by the bulk modulus of the water (Kw = 2.2.106 kPa)

• In the course of the dynamical action, the model generates additional pore pressure in the tail layers below the WL. The pore pressure generated does not have cumulative value over time during the earthquake. The model has the ability to register the value at any given moment that would appear at every step during the calculation. This is the reason why the resulting pore water pressure should be considered approximate.

• For the finite element mesh, a 15 nodal triangular finite element is used. A criterion of Kuhlemeyer & Lysmer (1973) [18] for dynamic analysis is applied to determine the mesh size, which has an average size of finite element L_{ave} should not exceed 1/8 of the wavelength λ i.e. $L_{ave} \leq \lambda / 8 = V_{Smin} / (8 f_{max})$, where: $V_{s,min}$ V_s, min is the minimum wave velocity in soil deposit; f_{max} - maximum frequency of the action.

The selection of seismic actions in the form of accelerograms for verification of the dynamic analysis is subject to the following criteria:

- Analysis with real accelerograms typical for the region with predominant frequency, as close as possible to the first natural frequency of the soil deposits f_I (for the tailings dam up to 830.0 m f_I = 0.83 Hz) scaled for different return periods (TR).
- Analysis with accelerograms generated by the RSHA method / PSHA / for different return periods (TR), with a predominant frequency as close as possible to the first natural frequency of the soil deposits f_I.
- Analysis with synthetic accelerograms generated by the deterministic approach / DSHA /, with a predominant frequency as close as possible to the first natural frequency of the soil deposits f_1.
- The accelerograms of Figs. 4, Fig.5 and Fig. 6. are used.

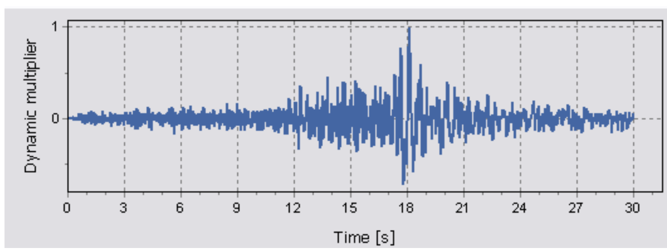

Fig. 4. Pernik EW AQ085 2Hz; PGA=0,4g (TR =10000г.); PGA=0,177g (TR =1000г.)

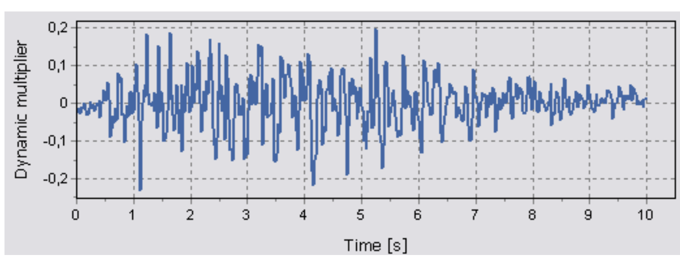

Fig. 5. DDD8 magnitude M7,0; D15; Vs=800m/s; 5 Hz; PGA=0,23g

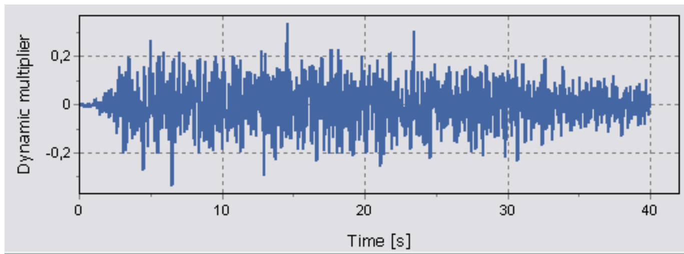

Fig. 6. N3 Vs=1000m/s, TR=10000г.; 5 Hz; PGA=0,332g

3. RESULTS

The results of the calculations are summarized in Table. 3 and are shown in Fig. 7- Fig. 11.

Table 3. Maximal displaxements u_{max}, accelerations a_{max} deviatoric deformations $\gamma_{s,max}$

Акселерограма	*PGA* (g)	Динамично време (s)	$\lvert u_{max} \rvert$ (cm)	a_{max} /*PGA*	$\gamma_{s,max}$ (%)
Pernik-10 000	0,400	30	21	0,86	0,3
Pernik-1000	0,177	30	7	1,3	0,1
DDD8	0,230	10	8,5	0,91	0,2
N3	0,332	40	42	1,0	0,3

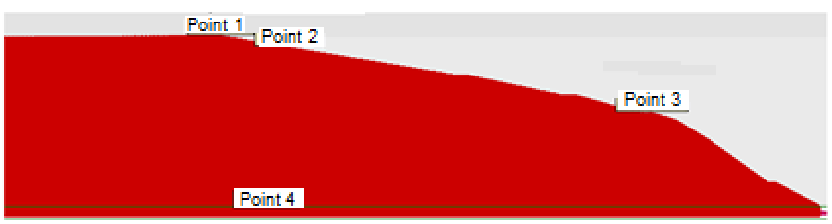

Fig. 7. Specific points for results

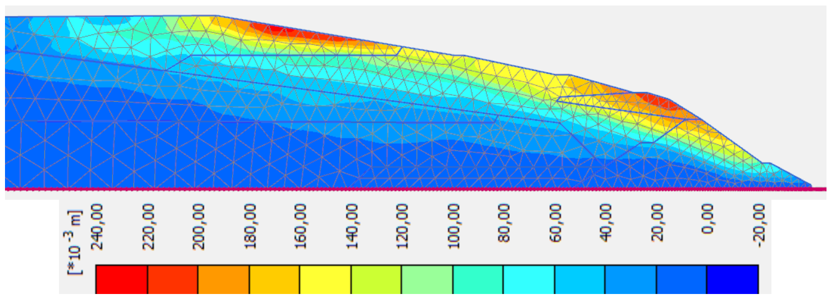

Fig. 8. Horizontal displacement accelerograms Pernik, PGA=0,4g

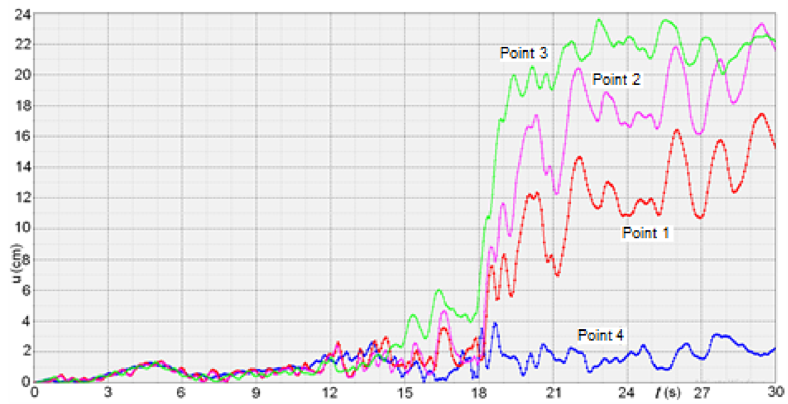

Fig. 10. Displacement (*u*,cm) /Time (*t,* s) of the points of (Fig. 9) accelerogram Pernik, PGA=0,4g

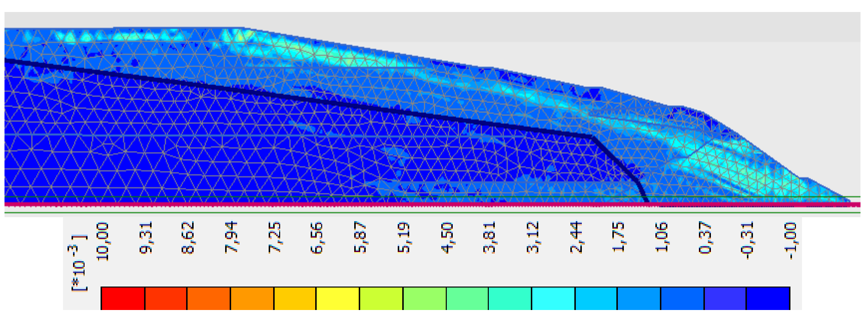

Fig. 11. Deviatoric strains accelerograms Pernik, PGA=0,4 g

From the analysis of the results, the following conclusions were made:

- The maximum displacements u_{max} in the main wall are reached in an area along the inclined part of the tailings dam deposits, with peak values being obtained slightly below the apex of the slope and at the top of the boulder dam. The horizontal displacements are about 40 cm.
- For the main dam, the maximum accelerations a_{max} are reached in the areas at the top of the slope. As an example, they are close to the maximum PGA amplitude of the input accelerograms. Amplification of PGA accelerations is observed by a maximum of 30% for the Pernik -1000 earthquake (with the smallest amplitude) due to the more elastic reaction of the deposit.
- Deviatoric deformations $\gamma_{s,max}$ (maximal shear deformations) trace the potential failure zones in the tailings dam structure. Values of $\gamma_s > 1\%$ are indicative of failure (Ishihara 2003 [7]). For the main dam, deviatoric deformations were obtained with values of $\gamma_{s,max} < 0.5\%$. For the cut-off wall, deformations of $\gamma_{s,\ max} > 1\%$ are observed in the local contact zone between the core of the wall and the boulder dam, which indicates that the two materials slip towards each other. Maximum deviatoric deformations occur mainly in the clay core due to its much lower rigidity and shear strength compared to the shear resistance of the boulder dam. The values there are $\gamma_{s,\ max} = 0.4 - 0.8\%$.

CONCLUSIONS

The analysis of the seismic behaviour of the Liulyakovitsa tailings dam appears to be relevant in assessing the stability of the facility. The analysis is based on a modern multi-parameter computer model based on FEM, in which the simulation of seismic action and seismic response is sufficiently consistent with the actual behaviour of this earth structure.

REFERENCES

[1] Das, B., M., (1993). Principles of soil dynamics, PWS-KENT Publishing Company, 293 p.

[2] Hamova, M., (2005). Development of soil dynamics, magazine “Construction”, No. 5.

[3] Hardin, B. O., Drenvich, V. P. (1972a). Shear modulus and damping in soil: design equation and curves. Jour. of the Soil Mech. and Found. Division, ASCE, 98 (SM7).

[4] Hardin, B. O., Drenvich, V. P. (1972b). Shear modulus and damping in soil: Measurement and parameter effects. Jour. of the Soil Mech. and Found. Division, ASCE, 98 (SM6).

[5] Hashash, Y., Park, D. (2002) Viscous damping formulation and high frequency motion propagation in non-linear site response analysis. Soil dynamic earthquake engineering, 22 (7), pp. 611-624.

[6] Hudson, M., Idriss, I. M., and Beikae, M. (2003). QUAD4M : A computer program to evaluate the seismic response of soil structures using finite element procedures and incorporating a compliant base. rev. 2003, Center for Geotechnical Modeling Dept. of Civil and Environmental Engineering University of California Davis.

[7] Ishihara, K. (2003) Soil Behaviour in Earthquake Geotechnics. Oxford Univ. Press Inc., New York.

[8] Kramer, St., (1996). Geotechnical Earthquake Engineering, Prentice-Hall, Inc. Simon&Schuster, 673p.

[9] Kerenchev, N., (2012-2013). Determining the dynamic modulus and dynamic settlement for the "New Lead Processing" foundation – KCM Plovdiv.
[10] Kerenchev, N., (2013-2014). Developing an experimental laboratory setting for determining soil parameters related to deformation. Annual of the University of Architecture, Civil Engineering and Geodesy, Fascicule IV, Geotechnical Engineering, Vol. XLVI, Sofia.
[11] Kerenchev, N. (2015). Analysis of seismic slope stability and deformations. Dissertation for the degree of PhD, University of Architecture, Civil Engineering and Geodesy, Sofia.
[12] Kerenchev, N., (2019). On the E50 modulus of tailing dams materials. 19th Int. Multidisciplinary Scientific Geoconference SGEM2019.
[13] Kerenchev, N., Milev, N., (2019). Assessment of the Dynamic Soil Properties for the FEM Model of the Lyulyakovitsa Tailings Dam. Eighth Geotechnics in Civil Engineering Conference, Vrnjačka Banja (Serbia).
[14] Kerenchev, N., Mihova, L., Bonev, Z., Kisliakov, D., (2018). Approaches for estimation of the performance factor for tailing dams. XVIII Anniversary Int. Scientific Conf. by Construction and Architectre VSU'2018, Sofia.
[15] Kostova, St., (2011). Principles for determining of the soil ground bearing capacity according to Eurocode 7. Academic journal Mechanics, Transport, Communications, Issue 2, No./ Aricle ID: 00494, http://www.mtc-aj.com.
[16] Kostova, St., (2011). Designing Methods of the Bearing Capacity of the Soils according to Eurocode 7 and Bulgarian Norms. Academic journal, Mechanics, Transport Communications ISSN 1312-3823 (print), ISSN 2367-6620 (online), http://www.mtc-aj.com, article № 0550, issue 3/3, pp.V-89-V-95.
[17] Kostova, St., (2018). Analysis of the procedure for designing of the bearing capacity of the soils according to Eurocode 7, Academic Journal Mechanics, Transport, Communications, art. ID:1558 p.XIV-16- XIV-23, Vol. 16, No. 1/3.
[18]Kuhlemeyer, R. L., Lysmer, J. (1973) Finite element method accuracy for wave propagation problems. Jour. of Soil Mech. and Found. Division, 99 (5), pp. 421-427.
[19] Mihova, L., Kerenchev, N., (2013-2014). Shear strength of clays in dynamic loading: Part 1. Correlations. Annual of the University of Architecture, Civil Engineering and Geodesy, Fascicule IX-B, Scientific Research – II, Vol. XLVI, Sofia.
[20] Mihova, L., Kerenchev, N., (2013-2014). Shear strength of clays in dynamic loading: Part 2. Analysis for clay of Sofia town area. Annual of the University of Architecture, Civil Engineering and Geodesy, Fascicule IX-B, Scientific Research – II, Vol. XLVI, Sofia.
[21] Milev, N., (2017). Small-Strain Behaviour of Cohesionless Soils by Triaxial Tests and Dynamic Measurement Methods - Seventh Geotechnics in Civil Engineering Conference, Šabac (Serbia).
[22] Milev, N., (2018). Laboratory Shear Wave Velocity Evaluation of Sofia Sofia Sand by Means of Bender-Elements. Eighteenth Anniversary International Scientific Converence by Construction and Architecture VSU Lyuben Karavelov, Sofia.
[23] Milev, N. (2018). Assessment of Soil Liquefaction Potential of Reconstituted Samples of Sofia Sand From Undrained Cyclic Triaxial Tests. Sixth International Conference on Earthquake Engineering and Engineering Seismology, Kraljevo (Serbia).
[24] Milev, N., (2018). Static and Dynamic Evaluation of Elastic Properties of Sofia Sand and Toyoura Sand by Sophisticated Triaxial Tests. Journal for Research of Materials and Structures (ISSN 2217-8139), Belgrade (Serbia).

[25] Milev, N., (2019). Experimental Evaluation of Shear Wave Velocity Change Induced by Repeated Liquefaction of Sofia Sand by Undrained Cyclic Triaxial Tests - International Conference on Earthquake Geotechnical Engineering (ICEGE 2019), Rome (Italy).
[26] PLAXIS, Material Models Manual. (2015).
[27] Rayleigh, J. W. S., Lindsay, R. B. (1945). The theory of sound, Dover Publications, New York.
[28] Seed, H. B., Idriss, I. M. (1970). Soil moduli and damping factors for dynamic response analyses. University of California, Berkeley, Report No. EERC 70-10.
[29] Sulay, I., (2019). Basic principles for geotechnical design in the updated part "Soil Body" of the Standard No. RD-02-20-2/28.08.2018 for road design. Annual of the University of Architecture, Civil Engineering and Geodesy, Vol. 52, Fasc. 2, Sofia
[30][22] Sulay, I., Tanev, T., (2016). Stability of the road soil body – practical investigation according regulations of Standard for Road Design and Eurocode, Magazine "Transportation Engineering & Infrastructure", No. 13.
[31] Vucetic, M., Dobry, R. (1991). Effect of soil plasticity on cyclic response. Journal of Geotechnical Engineering, ASCE, Vol. 117. No. 1.